Carbohydrate Polymers 82 (2010) 62–68

Contents lists available at ScienceDirect

Carbohydrate Polymers

journal homepage: www.elsevier.com/locate/carbpol

# Hydrogels prepared from pineapple peel cellulose using ionic liquid and their characterization and primary sodium salicylate release study

Xiuyi Hu, Kai Hu, Linlin Zeng, Mouming Zhao, Huihua Huang*

*Department of Food Science and Technology, South China University of Technology, Wushan Road 381, Guangzhou, Guangdong Province 510641, China*

ARTICLE INFO

*Article history:*
Received 4 February 2010
Received in revised form 11 April 2010
Accepted 13 April 2010
Available online 20 April 2010

*Keywords:*
Hydrogels
Pineapple peel cellulose
Ionic liquid
Characterization
Polyvinyl pyrrolidone

ABSTRACT

Hydrogels and polyvinyl pyrrolidone (PVPP) composite hydrogels were prepared from pineapple peel cellulose with 1-allyl-3-methylimidazolium chloride via different heating and cooling processes. The prepared hydrogels were characterized via the methods of texture profile analysis, Fourier infrared transform, X-ray diffraction, thermogravimetry analysis, differential scanning calorimetry and field emission scanning electron microscope. Swelling kinetics of the prepared hydrogels and their release kinetics were also compared in vitro with sodium salicylate (NaSA) as model drug. The results showed the hydrogels and PVPP-doped composite hydrogels exhibited differences in characterizations and NaSA release. PVPP increased the mechanical properties and thermal stability of the composite hydrogels. The freeze-dried hydrogels exhibited higher equilibrium swelling ratio and NaSA load ratio than the oven-dried hydrogels. PVPP addition decreased the equilibrium swelling ratio and NaSA load ratio of the freeze-dried hydrogels but increased those of the oven-dried hydrogels. Oven-drying processing and PVPP were propitious for slowing NaSA release.



## 1. Introduction

Cellulose from plants consists of anhydroglucopyranose units bound by β-(1 → 4)-glycosidic linkage and accordingly is described as the linear-polymer glucan with uniform chain structure (Fengel & Wegener, 1984). As the most abundant natural polymer in the world, cellulose possesses non-toxic, renewable, biodegradable and biocompatible characteristics. However, cellulose is difficult for processing in most solvents because of its insolubility resulted from its strong intra- and inter-molecular hydrogen bonding (Klemm, Heublein, Fink, & Bohn, 2005). Hence the extension of cellulose utilization is limited. Recently, an innovative class of green solvent, the room temperature ionic liquid has been developed as the alternative solvent for cellulose processing owing to its excellent dissolving capability, recyclability and negligible vapor pressure (EI Seoud, Koschella, Fidale, Dorn, & Heinze, 2007; Murugesan & Linhardt, 2005). For example, the ionic liquids with imidazolium structure, 1-butyl-3-methylimidazolium chloride (BMIMCl) and 1-allyl-3-methylimidazoliumchloride (AMIMCl) are used to dissolve and process cellulose into gels and composite materials for applications in controlling release of medicine and fertilizer (Kadokawa, Murakami, & Kaneko, 2008a; Kadokawa, Murakami, & Kaneko, 2008b; Kadokawa, Murakami, Takegawa, & Kaneko, 2009; Murakami, Kaneko, & Kadokawa, 2007; Murugesan & Linhardt, 2005; Prasad, Kaneko, & Kadokawa, 2009; Prasad, Murakami, et al., 2009; Swatloski, Spear, Holbrey, & Rogers, 2002; Wu et al., 2004; Zhang, Wu, Zhang, & He, 2005). In particular, as a powerful cellulose solvent, AMIMCl has been used to prepare various cellulose derivatives and cellulose-based materials such as hydrogels (Cao et al., 2007; Li, Lin, Yang, Wan, & Cui, 2009; Li, Wu, Liu, & Huang, 2009; Prasad, Kaneko, et al., 2009; Prasad, Murakami, et al., 2009; Zhang et al., 2007, 2005). The hydrogels prepared from plant fibers belong to three-dimensional cross-linked polymer and possess strong ability to imbibe and hold water within their three-dimensional cross-linked structures. Such cellulose derivatives show various potential biomedical applications, such as the soft contact lenses, wound dressing, super-absorbents and drug delivery systems based on their perfect hydrophilic nature (Gin, Dupuy, Baquey, Baquey, & Ducassou, 1990; Matthew, Salley, Peterson, & Klein, 1993; Mishra, Datt, Pal, & Banthia, 2008). Pineapple (*Ananas comosus* L. *Merryl*) is a typical tropic fruit with unique flavor widely grown in tropic regions. During can fruit and juice processing, pineapple peel is usually discharged before or after bromelain is extracted. Both the discharges of pineapple peel in these two ways produce waste about 35% of the full fruit and lead to serious environmental pollution. Pineapple peel is principally consisted of cellulose, hemi-cellulose, lignin and pectin (Bardiya, Somayaji, & Khanna, 1996). From the points of the view of

* Corresponding author. Tel.: +86 20 87112851; fax: +86 20 87113914.
*E-mail address:* fehhuang@scut.edu.cn (H. Huang).

0144-8617/$ – see front matter © 2010 Elsevier Ltd. All rights reserved.
doi:10.1016/j.carbpol.2010.04.023

multipurpose utilization and environmental protection, modification and utilization of pineapple peel cellulose are of important significance. This research mainly focused on the preparation of pineapple peel cellulose hydrogel (PPCH) with AMIMCl as the solvent of the extracted pineapple peel cellulose (PPC) and the preparation of composite pineapple peel cellulose hydrogel with the insoluble polyvinyl pyrrolidone (PVPP) as additive. Meanwhile the prepared hydrogels were characterized and the swelling kinetics of the prepared PPCH and its release kinetics were also investigated with sodium salicylate (NaSA) as the model drug.

## 2. Materials and methods

### 2.1. Preparation of PPC

To extract PPC, 30 g of pineapple peel was treated with 600 mL distilled water at 80 °C for 2 h. The insoluble residue was then delignified with sodium chlorite at pH 3.8–4.0 and 75 °C for 2 h. After collection through filtration, the residue was washed respectively with distilled water and ethanol and then was dried in a cabinet oven at 50 °C for 16 h. The dried residue was extracted with 400 mL of KOH (10%, w/v) at room temperature for 10 h to remove semi-cellulose and other impurities. After filtration, the residue was washed thoroughly with distilled water until the filtrate turned to neutral, and then was washed with ethanol (95%, v/v). PPC was obtained after the washed residue was dried in an oven at 50 °C for 16 h (Liu et al., 2007). The weight ratio of PPC extracted from pineapple peel by the above process is about 22%.

### 2.2. Preparation of PPCHs and the composite hydrogels

The hydrogels of PPC and their composite hydrogels were prepared from the extracted PPC via two processing methods: heating–cooling–washing process and heating–cooling–freezing–thawing–washing process (Kadokawa et al., 2009, 2008b; Li, Lin, et al., 2009; Li, Wu, et al., 2009; Prasad, Kaneko, et al., 2009; Prasad, Murakami, et al., 2009). In the case of heating–cooling–washing process, samples of PPC were weighed 0.5 g, 1 g and 1.5 g respectively and stir-treated with 20 g of AMIMCl (purchased from Shanghai Cheng Jie Chemical Co. Ltd., China) at 100 °C for 12 h in a shaker until to complete dissolution. Accordingly the PPC concentrations in the solutions were marked as 2.5%, 5% and 7.5% (w/w) respectively. PPC hydrogels formed after the solutions were cooled to ambient temperature. The excessive ionic liquid leached out from the hydrogels was rinsed out with distilled water. The obtained PPC hydrogels were respectively marked as PPCH2.5, PPCH5 and PCH7.5. The composite hydrogels of PPC were prepared via the same method by the addition of PVPP (purchased from Tokyo Chemical Industry Co., Ltd., Japan), where 5% of PPC and PVPP in AMIMCl were used and the formed hydrogel was marked as PVPP–PPCH.

In the case of heating–cooling–freezing–thawing–washing process, a solution of AMIMCl contained PPC and PVPP (5% each) was stir-treated at 100 °C for 12 h in a shaker until to complete dissolution. After cooled to ambient temperature, the obtained hydrogels were subjected to a six-cycle-treatment of freezing–thawing (frozen at −20 °C for 12 h and thawed at ambient temperature for 12 h). After the freezing–thawing treatments, the excessive ionic liquid leached out from the hydrogels was rinsed out with distilled water. The formed composite hydrogels in this way was marked as PVPP–PPCH-FT.

For characterization, swelling kinetics and in vitro release kinetics study, the obtained PPCH and their composite hydrogels were subjected to freeze-drying or oven-drying (50 °C for 12 h).

### 2.3. Characterization of PPCH and the composite hydrogels

Texture profile analysis (TPA) on the prepared PPCH and the composite hydrogels were performed according to the reported method (Bourne, 1982; Lin, Wang, & Wu, 2009). A TA-XT2i® Texture Analyzer (Stable Microsystems, Surrey, UK) equipped with a 5 kg load cell was used. Each sample of the hydrogels (clipped as 0.8 cm long and 2.5 cm in diameter) was subjected to two cycle compression to 30% of their initial length at a constant pre-speed of 5 mm $s^{-1}$, cross-head speed of 1 mm $s^{-1}$ and post-speed of 5 mm $s^{-1}$ via a cylindrical stainless steel probe (P5: 5 mm DIA CYLinDer Stainless). All measurements were duplicated 6 times. The TPA parameters of the prepared hydrogels including hardness, springiness, cohesiveness, gumminess and resilience were computed via the supplied Texture Expert software. The freeze-dried or oven-dried PPCH5, PVPP–PPCH and PVPP–PPCH-FT were characterized by Fourier transform infrared (FTIR), X-ray diffraction (XRD), thermogravimetry analysis (TGA), differential scanning calorimetry (DSC) and field emission scanning electron microscope (FESEM) respectively. The FTIR spectra were recorded from 4000 to 400 $cm^{-1}$ at a resolution of 2 $cm^{-1}$ and 32 scans per sample with FTIR Spectrometer (Vector 33, Bruker, Germany). The Wide-angle X-ray diffraction patterns were recorded on an X-ray diffraction (model D/max-IIIA, RIGAKU, Japan), in which Cu Ka radiation ($\lambda$ = 1.5406 Å) was used at 40 kV and 30 mA and the scanning speed was set at 2° $min^{-1}$ in the region of the diffraction angle ($2\theta$) from 4° to 60°. TGA and DSC patterns were recorded on a simultaneous thermal analyzer (NETZSCH STA449C, Germany) at a heating rate of 10 °C/min between 30 °C and 500 °C under $N_2$ atmosphere. FESEM images of the samples were recorded on an ultra-high resolution field emission scanning electron microscope (NoVaTM Nano SEM 430, Netherlands). The samples surfaces were gold-coated before observation.

### 2.4. Determinations of equilibrium swelling ratio (ESR) and swelling kinetics

The routine gravimetric method was adopted to determine the ESR of the prepared hydrogels (Chen, Liu, Liu, & Ma, 2009). Swelling study was performed in water at room temperature. The weighed dried hydrogel samples were immersed and got swollen in water for 3 days at room temperature so as to reach equilibrium status. After removal of the excess water on the surface via wet filter paper, the swollen hydrogel samples were weighed. All of the experiments were conducted in triplicate. ESR was calculated as follows:

$$\text{ESR}\ (\%) = \frac{W_s - W_d}{W_d} \times 100 \quad (1)$$

where $W_s$ is the weight of the swollen hydrogel samples at swollen equilibrium status and $W_d$ is the weight of the hydrogel samples prior to swelling. To record the swelling kinetics of the hydrogels, the immersed hydrogels in water were sampled at a regular interval and the ESR at time $t$ was calculated according to Eq. (1).

### 2.5. In vitro release kinetics of the prepared hydrogels

NaSA was used as the model drug for drug loading and release experiments on the prepared hydrogels. During the experiments, the dried hydrogels were incubated and equilibrated in the vials filled with 20 mL of NaSA aqueous solution (10%, w/v) for 2 weeks at ambient temperature. After incubation, the drug-loaded hydrogel samples were removed from NaSA aqueous solution and were rinsed twice with distilled water. The drug-loaded hydrogel samples were then vacuum-dried to constant weight at room temperature. The residual NaSA content in the solutions was determined with a Shimadzu ultraviolet–visible spectrophotome-

**Table 1**
The TPA parameter comparison between different hydrogels prepared from pineapple peel cellulose.

| Hydrogels | Hardness (g) | Springiness | Cohesiveness | Gumminess (g) | Resilience |
|---|---|---|---|---|---|
| PPCH2.5 | 323.59 ± 67.83[d] | 0.86 ± 0.04[a] | 0.50 ± 0.03[a] | 161.85 ± 38.69[d] | 0.41 ± 0.04[c] |
| PPCH5 | 1140.77 ± 109.81[c] | 0.89 ± 0.02[a] | 0.54 ± 0.02[a] | 617.61 ± 42.72[c] | 0.55 ± 0.03[a] |
| PPCH7.5 | 2117.67 ± 150.86[a] | 0.91 ± 0.01[a] | 0.53 ± 0.02[a] | 1122.48 ± 90.93[a] | 0.58 ± 0.01[a] |
| PVPP–PPCH | 1626.11 ± 444.83[b] | 0.88 ± 0.01[a] | 0.49 ± 0.03[a] | 776.53 ± 175.41[b] | 0.40 ± 0.01[c] |
| PVPP–PPCH-FT | 2211.45 ± 34.48[a] | 0.87 ± 0.01[a] | 0.50 ± 0.01[a] | 1109.13 ± 16.94[a] | 0.49 ± 0.01[b] |

[abcd]Values in a column with the same superscript mean not significantly different ($P < 0.05$).

ter according to the method reported by Demir et al. (2008). NaSA load ratios (%) of the prepared hydrogel samples were calculated based on Eq. (2):

$$\text{NaSA load ratio}\,(\%) = \frac{C_o V_o - C_t C_t}{m} \quad (2)$$

where $m$ is the mass of the hydrogel samples prior to loading. $C_o$ and $V_o$ are the concentration and volume of the NaSA solutions prior to loading respectively. $C_t$ and $V_t$ are the concentration and volume of the NaSA solution after loading respectively (Chen et al., 2009).

For drug release kinetics experiments, the drug-loaded hydrogel samples were transferred into 200 mL of distilled water (as the dissolution medium) and were stir-treated at 37 °C in a shaker. During the release, 5 mL of the dissolution medium was sampled at intervals for drug concentration determination; meanwhile an equal volume of distilled water was pipetted back to the dissolution medium so as to maintain the dissolution medium volume constant. The release percentage of drug was calculated according to the following equation:

$$\text{Cumulative amount released}\,(\%) = \frac{W_t}{W_{total}} \times 100 \quad (3)$$

where $W_t$ is the amount of the released drug at time $t$ and $W_{total}$ is the total adsorbed amount of the drug in hydrogel samples.

### 2.6. Statistical analysis

Analysis of variance and Duncan's multiple range tests were performed by using the Statistical Analysis System (SAS Institute, 1998). A value of $P < 0.05$ was regarded as significantly different.

## 3. Results and discussion

### 3.1. Texture profile comparison between the prepared hydrogels

Table 1 shows the TPA of different hydrogels prepared from PPC. From Table 1, it was observed that the springiness and cohesiveness among the prepared PPC hydrogels were maintained unchanged basically. However for the hydrogels of PPCH2.5, PPCH5 and PPCH7.5, the hardness, gumminess and resilience were found significantly increased with the increase of PPC content. Compared with PPCH2.5 and PPCH5, the composite hydrogel, PVPP–PPCH exhibited significant increase in hardness and gumminess, indicating the enhancement effect of PVPP on the hydrogels in texture and mechanical properties. However, in virtue of higher cellulose content, PPCH7.5 exhibited the even higher hardness, gumminess and resilience than PVPP–PPCH. After the cycle freezing–thawing processing, PVPP–PPCH-FT was found exhibiting higher hardness, gumminess and resilience than PVPP–PPCH, but no obvious changes in springiness and cohesiveness were observed, indicating the improvement effect of the cycle freezing–thawing process on the composite hydrogel in texture profile and mechanical properties.

### 3.2. FTIR analysis

As a comparison, the FTIR spectra of PPC, PVPP and freeze-dried hydrogels of PPCH5, PVPP–PPCH and PVPP–PPCH-FT are shown in Fig. 1. From Fig. 1a, it was observed that PPC exhibited the absorption peaks at 3411 and 2914 $cm^{-1}$ which represent the O–H stretching of polymeric compounds and the characteristic vibration of C–H stretching respectively. PPC also showed the absorption peaks in the fingerprint regions at 1431, 1165 and 1032 $cm^{-1}$ which are attributed to the cellulose structure (During, 1991; Silverstein, Bassler, & Morrill, 1981; Wang, Han, & Zhang, 2007). For PVPP, the band at 1658 $cm^{-1}$ due to the C=O stretching mode was observed (Fig. 1b). PVPP also showed fairly strong absorption in 1500–1370 $cm^{-1}$ region, which are the contributions mainly from the C–H bending of $CH_2$ and CH moieties. The absorption bands of PVPP at 1319, 1291 and 1226 $cm^{-1}$ were also observed, which is perhaps attributed to the C–N stretching likely coupled with the C–H bending mode (Patel & Chaudhuri, 2009). Compared with PPC, the FTIR spectrum bands of PPCH5 were found shifted to 3424, 2917, 1642, 1425, 1325, 1160, 1068 and 1024 $cm^{-1}$ respectively from 3411, 2914, 1638, 1431, 1320, 1165, 1060 and 1032 $cm^{-1}$ (Fig. 1c), suggesting the existence of interaction between PPC and AMIMCl. Compared with PPC and PVPP, the spectrum of PVPP–PPCH exhibited the overlapped characterization from PPC and PVPP (Fig. 1d). Meanwhile, the bands at 3411 $cm^{-1}$ for PPC, at 3445 $cm^{-1}$ for PVPP were found overlapped and shifted to 3428 $cm^{-1}$ for PVPP–PPCH. The bands at 2914 $cm^{-1}$ for PPC, at 2956 $cm^{-1}$ for PVPP were found also overlapped and shifted to 2922 $cm^{-1}$ for PVPP–PPCH. The adsorption peeks at 1638 $cm^{-1}$ for PPC and at 1658 $cm^{-1}$ for PVPP were found overlapped at 1657 $cm^{-1}$ for PVPP–PPCH. The bands at 1264, 1237 $cm^{-1}$ for PPC and at 1226, 1172 $cm^{-1}$ for PVPP were found overlapped and shifted to 1230 $cm^{-1}$ for PVPP–PPCH. The bands at 1112, 1060, 1032 $cm^{-1}$ for PPC and at 1076, 1020 $cm^{-1}$ for PVPP were also

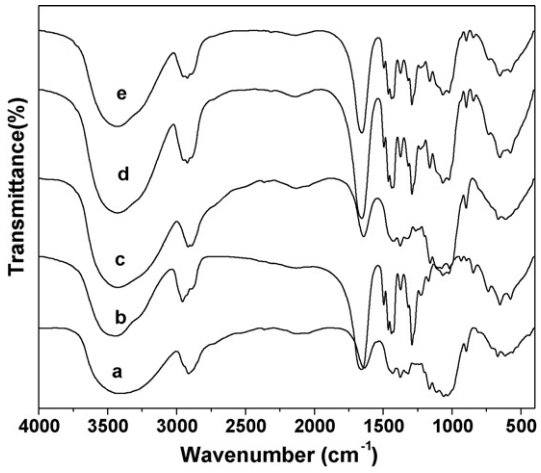


**Fig. 1.** FTIR spectra of PPC, PVPP and the freeze-dried hydrogels of PPCH5, PVPP–PPCH and PVPP–PPCH-FT. a stands for PPC, b for PVPP, c for PPCH5, d for PVPP–PPCH, e for PVPP–PPCH-FT.

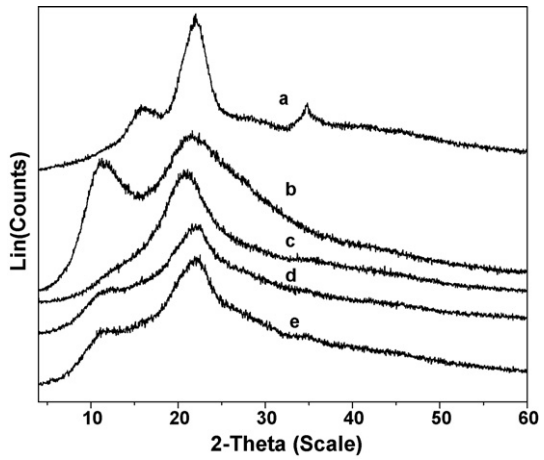


**Fig. 2.** XRD patterns of PPC, PVPP and the freeze-dried hydrogels of PPCH5, PVPP–PPCH and PVPP–PPCH-FT. a stands for PPC, b for PVPP, c for PPCH5, d for PVPP–PPCH, e for PVPP–PPCH-FT.

found overlapped and shifted to 1068, 1023 $cm^{-1}$ for PVPP–PPCH respectively. All of these changes suggest the existence of the interaction between PPC and PVPP in AMIMCl solution. However, little change was observed between the spectrum of PVPP–PPCH and PVPP–PPCH-FT (Fig. 1e), indicating that the hydrogel structure was little affected by the cycle freezing–thawing.

### 3.3. XRD analysis

The XRD curves of PPC, PVPP and the freeze-dried hydrogels of PPCH5, PVPP–PPCH and PVPP–PPCH-FT are shown in Fig. 2. The XRD profile of PPC in Fig. 2a was found exhibiting the typical diffraction peaks respectively at around 15°, 22° and 34° due to the crystal structure of cellulose I (Prasad, Kaneko, et al., 2009; Prasad, Murakami, et al., 2009). The XRD profile of PVPP in Fig. 2b was found exhibiting the typical diffraction peaks respectively at around 11° and 22° due to its crystal structure. But for PPCH5, the diffraction peaks were found disappeared at around 15° and 34° (Fig. 2c). For PVPP–PPCH and PVPP–PPCH-FT, the diffraction peaks were found markedly weakened (Fig. 2d and e). These XRD changes indicate that the crystal structures of PPC and PVPP are subject to disruption largely when they are turned into PPCH5 and composite hydrogels due to the breaking of hydrogen bonds which are responsible for the crystallinity (Kadokawa et al., 2009; Prasad, Kaneko, et al., 2009; Prasad, Murakami, et al., 2009).

### 3.4. Thermal analysis

The thermal analysis including TGA and DSC on PPC, PVPP and the freeze-dried hydrogels of PPCH5, PVPP–PPCH and PVPP–PPCH-FT are shown in Fig. 3. PPC was observed possessing two endothermic peaks at 80.7 °C and 354.2 °C respectively on the DSC curve (Fig. 3a) and exhibiting the weight loss in two phases correspondingly on the TGA curve (Fig. 3a). Thereinto, the first phase commenced between 54.8 °C and 108.5 °C and the weight loss was about 6.34%, corresponding with the endothermic peaks at 80.7 °C on its DSC curve. Maybe this is attributed to the loss of the adsorbed water and bound water in the cellulose (Simi & Abraham, 2010). The second phase of the weight loss commenced at 324.5 °C and continued up to 365.9 °C and the weight loss was about 70.89%, corresponding with the endothermic peak at 354.2 °C on its DSC curve. This is perhaps attributed to the degradation of PPC. From Fig. 3b, it was found that PVPP exhibited higher thermal stability than PPC and the weight loss was found increased steeply with the increase of temperature. On the TGA curve of PVPP, the first phase was found

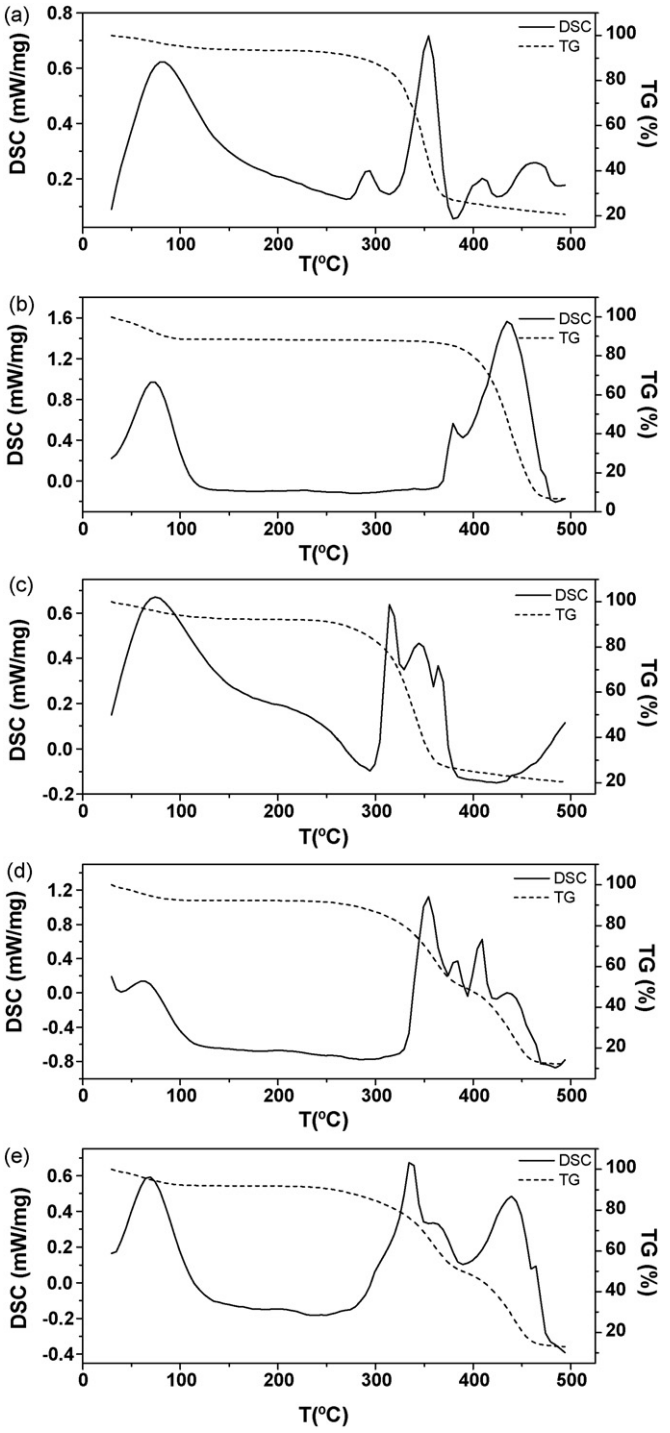


**Fig. 3.** TGA and DSC patterns of PPC, PVPP and the freeze-dried hydrogels of PPCH5, PVPP–PPCH and PVPP–PPCH-FT. a stands for PPC, b for PVPP, c for PPCH5, d for PVPP–PPCH, e for PVPP–PPCH-FT.

between 57.0 °C and 89.1 °C and the weight loss was about 11.49%. The second phase took place from 408.8 °C to 460.3 °C, thereinto the maximum decomposition rate was found at 437.2 °C, corresponding with the endothermic peaks on its DSC curve. The weight loss during this phase was about 81.46%. From Fig. 3c, it was observed that that PPCH5 exhibited lower thermal stability than PPC and the weight loss of PPCH5 decreased only slightly with the increase of temperature. On the TGA curve of PPCH5, the first phase commenced between 53.5 °C and 91.3 °C and the weight loss was about 6.57%. The second phase was from 308.1 °C to 357.5 °C, thereinto

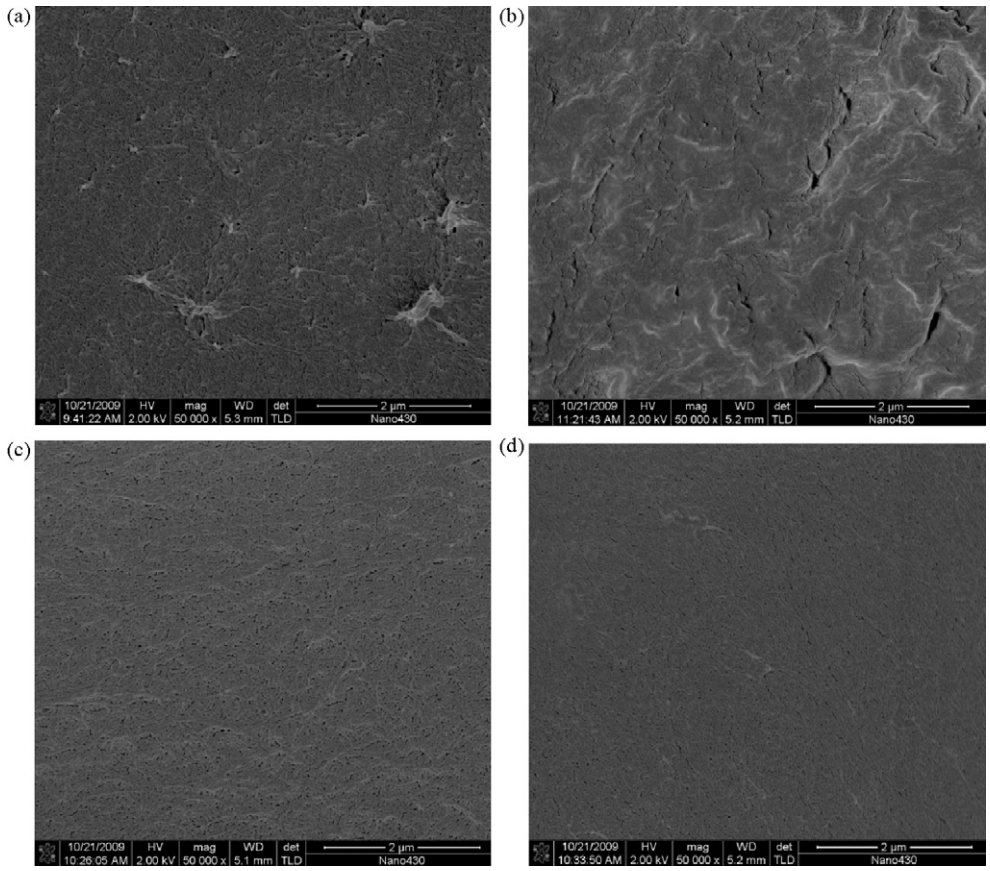


**Fig. 4.** FESEM images of different hydrogels prepared from pineapple peel cellulose. a stands for freeze-dried PPCH5, b for the oven-dried PPCH5, c for the freeze-dried PVPP–PPCH, d for the freeze-dried PVPP–PPCH-FT.

the three endothermic peaks were found at 313.4 °C, 344.4 °C and 365.3 °C respectively. As shown on the DSC curve of PPCH5, the maximum decomposition rate was observed at 313.4 °C and the weight loss corresponding with this phase was about 68.96%. These exhibitions of PPCH5 in thermal degradation also indicate the disruption of the crystal regions in PPCH5 cellulose (Kadokawa et al., 2009), as proven by the XRD analysis (Fig. 2).

Compared with PPCH5, PVPP–PPCH was found possessing higher thermal stability and its weight loss was divided in three phases on the TGA curve (Fig. 3d). The first phase was found between 45.2 °C and 83.4 °C and the weight loss was about 7.65%. The second phase commenced at 327.5 °C and continued up to 376.0 °C, in which, 39.43% weight loss was observed, corresponding with the endothermic peaks at 355.1 °C and 380.9 °C on its DSC curve. The third phase of the weight loss was found at 417.0 °C and up to 456.9 °C. During this phase, about 37.57% weight loss was observed (perhaps due to the degradation of PVPP in PVPP–PPCH), corresponding with the endothermic peaks at 406.9 °C and 437.6 °C on its DSC curve, indicating that there also is the disruption of the cellulose crystal regions and PVPP in PVPP–PPCH. However it is explicit that PVPP addition can significantly increase the thermal stability of hydrogels.

Compared with PVPP–PPCH, PVPP–PPCH-FT was found exhibiting slightly lower thermal stability. As shown in Fig. 3e, the weight loss of PVPP–PPCH-FT was found in three phases on the TGA curve. Thereinto, the first phase was found between 64.3 °C and 85.6 °C and the weight loss was about 7.37%. The second phase commenced at 315.6 °C and continued up to 375.6 °C and about 43.12% weight loss was observed (due to the degradation of PPC in PVPP–PPCH-FT), corresponding with the endothermic peaks at 333.8 °C and 359.6 °C on its DSC curve. The third phase was at 418.9 °C and up to 458.1 °C and about 35.69% weight loss was observed (due to the degradation of PVPP in PVPP–PPCH-FT), corresponding with the endothermic peaks at 437.4 °C on its DSC curve. These exhibitions indicate that the freezing–thawing process can change the thermal process of hydrogels and decrease their thermal stability slightly.

### 3.5. FESEM micrograph

Fig. 4 shows the FESEM micrographs of the freeze-dried and oven-dried PPCH5 (Fig. 4a and b), freeze-dried PVPP–PPCH (Fig. 4c) and freeze-dried PVPP–PPCH-FT (Fig. 4d). As the PVPP-undoped hydrogels, both the freeze-dried and oven-dried PPCH were observed possessing the rough bulging structures on their FESEM micrographs. Especially the cavity and cracks resulted from the superficial moisture evaporation were found very distinct in the oven-dried case (Fig. 4b). Moreover, uniform sub-micrometer pores were observed for the freeze-dried PPCH5 while no such structures was found for the oven-dried PPCH5, which perhaps is due to the hydrogel shrinkage during oven-drying. As the PVPP-doped hydrogels (i.e. composite hydrogels), PVPP–PPCH5 and PVPP–PPCH-FT were observed exhibiting comparatively more uniform and smaller sub-micrometer pores but no rough bulging structures on their FESEM micrographs (Fig. 4c and d), especially for the freeze-thawing samples (PVPP–PPCH-FT), indicating that freeze-drying is propitious for maintaining the intrinsic structure of hydrogels and PVPP is a perfect miscible medium for cellulose and AMIMCl during gelling. It is via these sub-micrometer pores that water is imbibed into the hydrogel structure. Since the ESR depends on the size of the sub-micrometer pores. Too big or too small sub-micrometer pores will impede the swelling of hydrogels. So PVPP in fact affects the ESR of the prepared hydrogels.

**Table 2**
Equilibrium swelling ratios (%), NaSA load ratios (%) of different hydrogels prepared from pineapple peel cellulose.

| Hydrogels | Drying process | Equilibrium swelling ratios (%) | NaSA load ratios (%) |
|---|---|---|---|
| PPCH5 | Freeze-dried | 486.67 ± 12.47[a] | 48.65 ± 1.15[a] |
| PVPP–PPCH | Freeze-dried | 400.00 ± 9.12[b] | 36.04 ± 0.95[b] |
| PVPP–PPCH-FT | Freeze-dried | 326.67 ± 6.72[c] | 28.00 ± 0.79[c] |
| PPCH5 | Oven-dried | 130.88 ± 2.20[e] | 2.35 ± 0.09[f] |
| PVPP–PPCH | Oven-dried | 178.67 ± 2.85[d] | 17.28 ± 0.27[d] |
| PVPP–PPCH-FT | Oven-dried | 173.33 ± 2.82[d] | 8.16 ± 0.25[e] |

[abcd]Values in a column with the same superscript are not significantly different ($P < 0.05$).

### 3.6. Equilibrium swelling ratios and swelling kinetics

Table 2 shows the measured ESR of the oven-dried and freeze-dried PPCH5, PVPP–PPCH and PVPP–PPCH-FT in water at room temperature. It was found that all of the freeze-dried hydrogels exhibited significant higher ESR than all the oven-dried hydrogels, suggesting freeze-drying process is propitious for maintaining the intrinsic structure of hydrogels. Compared with the freeze-dried PPCH5, the freeze-dried PVPP–PPCH and PVPP–PPCH-FT exhibited significant lower ESR. Compared with the oven-dried PPCH5, the oven-dried PVPP–PPCH and PVPP–PPCH-FT exhibited significant higher ESR. These results indicate that PVPP addition is propitious to decrease the ESR of the freeze-dried hydrogels but increase the ESR of the oven-dried hydrogels. As observed on the FESEM micrographs (Fig. 4), PVPP addition is propitious to form more compact and uniform structure and make the hydrogels possess comparatively smaller sub-micrometer pores during freeze-drying, especially for the freeze-dried hydrogels and freeze-thawing samples (PVPP–PPCH-FT). Because water is imbibed and restricted in the hydrogel structure via the smaller sub-micrometer pores and the ESR of hydrogels depends on the size of the sub-micrometer pores as the water imbiber. Too big or too small sub-micrometer pores do not benefit hydrogel swelling. Therefore, the swelling of various freeze-dried hydrogels is restricted and the ESR is accordingly decreased. However, compared with the freeze-dried PPCH5, the oven-dried PPCH5 showed few sub-micrometer pores on the FESEM micrograph due to the hydrogel shrinkage during oven-drying. Such a shrinkage phenomenon of hydrogel during oven-drying was also observed for the oven-dried PVPP–PPCH and PVPP–PPCH-FT. In fact, the shrinkage of the oven-dried PPCH5 was found more serious than the oven-dried PVPP–PPCH and PVPP–PPCH-FT. It is explicit that PVPP component in PVPP–PPCH and PVPP–PPCH-FT can weaken this shrinkage phenomenon during oven-drying. Consequently PVPP addition is propitious for the swelling of hydrogels and the oven-dried PVPP-doped hydrogels accordingly possess higher ESR than oven-dried PPCH5 (the PVPP-undoped hydrogels).

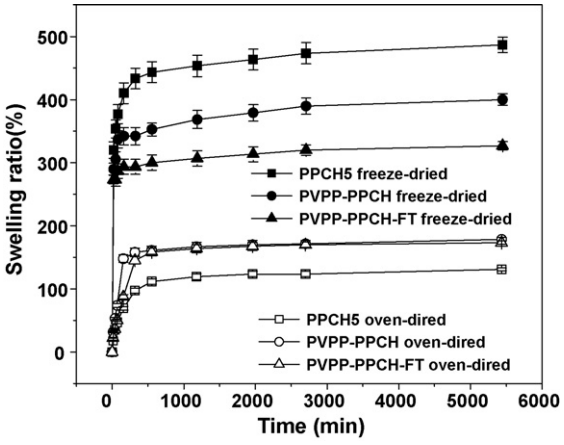


**Fig. 5.** The swelling kinetics of different hydrogels prepared from pineapple peel cellulose.

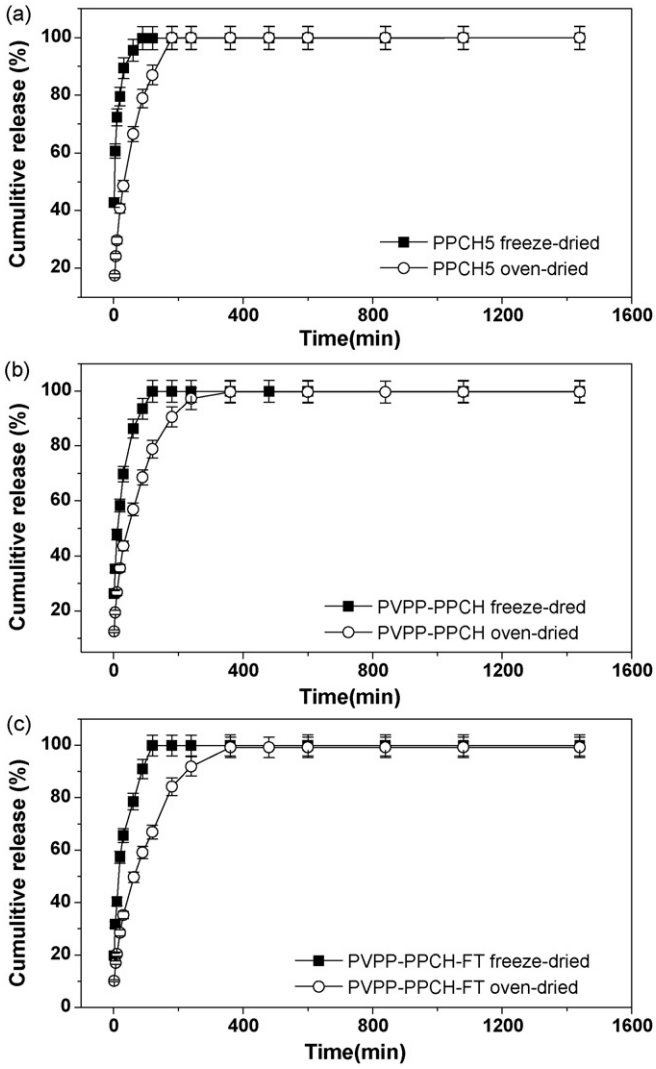


**Fig. 6.** The release kinetics of different hydrogels prepared from pineapple peel cellulose.

Fig. 5 shows the swelling kinetics of the freeze-dried and oven-dried PPCH5, PVPP–PPCH and PVPP–PPCH-FT in water at room temperature. The swelling rates of these hydrogels were found increased as time extended. Such an increase tendency was slowed notably after 540 min and the swelling equilibrium was after 2700 min basically.

### 3.7. NaSA load ratio and release kinetics

Table 2 also shows the NaSA load ratios (%) of the both oven-dried and freeze-dried PPCH5, PVPP–PPCH and PVPP–PPCH-FT. From the table, it was found that all of the freeze-dried hydrogels exhibited significant higher NaSA load ratios than all the oven-dried hydrogels. Maybe the distinct intrinsic structure and higher swelling capability are attributed to this phenomenon. From Table 2, it was found that PVPP addition could lower the NaSA load ratios of the freeze-dried hydrogels but increase the NaSA load ratios of the oven-dried hydrogels. These phenomena are similar to the case of ESR. The rational explanation is that PVPP affects the intrinsic structure of the hydrogels in the similar way. As shown on

the FESEM micrographs (Fig. 4), as a perfect miscible medium, PVPP makes the freeze-dried hydrogels more compact and uniform with smaller sub-micrometer pores during freeze-drying, especially for the freeze-thawing samples (PVPP–PPCH-FT). Hence PVPP addition restricts the swelling of the freeze-dried hydrogels and the NaSA-loading is lowered. However, PVPP addition can weaken the shrinkage of hydrogels during oven-drying. In this way, the restriction of the swelling of the oven-dried hydrogels is accordingly weakened. Consequently PVPP addition is propitious to increase the NaSA-loading of the oven-dried hydrogels.

For drug controlling release from a polymer matrix, some parameters are closely involved, such as the swelling behavior of polymer matrix, drug affinity to polymer chains, solubility of drug in water, drug change interval of release media, etc. (Brazel & Peppas, 1999; Chen et al., 2009). In this work, the effects of drying process and PVPP addition on the release kinetics of the hydrogels prepared from PPC were studied with NaSA as the model drug, exhibited as Fig. 6. All the hydrogels, including freeze-dried and oven-dried PPCH5, PVPP–PPCH and PVPP–PPCH-FT were observed exhibiting a linear steep phase and slow phase during NaSA release. The release ratios reached almost 99–100% at the end. For the freeze-dried PPCH5, the linear steep NaSA release was found within 90 min, however for the oven-dried PPCH5, the linear steep NaSA release was observed within 180 min (Fig. 6a). For the freeze-dried PVPP–PPCH, the linear steep NaSA release arose within 120 min, however for the oven-dried PVPP–PPCH, the linear steep NaSA release was extended to 360 min (Fig. 6b). For the freeze-dried PVPP–PPCH-FT, the linear steep NaSA release arose within 120 min while for the oven-dried PVPP–PPCH-FT, the linear steep NaSA release was extended to 360 min (Fig. 6c). These differences indicate that oven-drying processing and PVPP addition benefit for slowing the NaSA release and extending the release equilibrium time.

## 4. Conclusions

Hydrogels and composite hydrogels prepared from pineapple peel cellulose show differences in characterization and NaSA release. As a functional miscible medium, PVPP can improve the mechanical properties and thermal stability of the composite hydrogels. The freeze-dried hydrogels possess higher ESR and NaSA load ratios than the oven-dried hydrogels. PVPP addition makes the freeze-dried hydrogels decrease in ESR and NaSA load ratios but makes the oven-dried gels increase in ESR and NaSA load ratios. Oven-drying processing and PVPP addition are propitious for slowing the NaSA release.

## Acknowledgements

The authors thank the Ministry of Science and Technology of the People's Republic of China (2007AA100404) and The Department of Science and Technology of Guangdong Province, China for the financial support (Grant Nos. 2007498612, 2007B090100009, 2008A024200003).

## References

Bardiya, N., Somayaji, D., & Khanna, S. (1996). Biomethanation of banana peel and pineapple waste. *Bioresource Technology*, *58*(1), 73–76.

Bourne, M. C. (1982). Viscosity and consistency. In M. C. Bourne (Ed.), *Food texture and viscosity. Concept and measurement* (pp. 199–246). New York: Academic Press.

Brazel, C. S., & Peppas, N. A. (1999). Mechanisms of solute and drug transport in relaxing, swellable, hydrophilic glassy polymers. *Polymer*, *40*(12), 3383–3398.

Cao, Y., Wu, J., Meng, T., Zhang, J., He, J., Li, H., et al. (2007). Acetone-soluble cellulose acetates prepared by one-step homogeneous acetylation of cornhusk cellulose in an ionic liquid 1-allyl-3-methylimidazolium chloride (AmimCl). *Carbohydrate Polymers*, *69*(4), 665–672.

Chen, J., Liu, M., Liu, H., & Ma, L. (2009). Synthesis, swelling and drug release behavior of poly(N,N-diethylacrylamide-co-N-hydroxymethyl acrylamide) hydrogel. *Materials Science and Engineering: C*, *29*(7), 2116–2123.

Demir, S., Kahraman, M. V., Bora, N., Apohan, N. K., Scedil, A., & Ogan, E. (2008). Preparation, characterization, and drug release properties of poly(2-hydroxyethyl methacrylate) hydrogels having beta-cyclodextrin functionality. *Journal of Applied Polymer Science*, *109*(2), 1360–1368.

During, J. R. (1991). *Vibrational spectra and structure*. New York: Elsevier.

El Seoud, O. A., Koschella, A., Fidale, L. C., Dorn, S., & Heinze, T. (2007). Applications of ionic liquids in carbohydrate chemistry: A window of opportunities. *Biomacromolecules*, *8*(9), 2629–2647.

Fengel, D., & Wegener, G. (1984). *Wood: Chemistry, ultrastructure, reactions*. Berlin/New York: Walter de Gruyter., pp. 613–635.

Gin, H., Dupuy, B., Baquey, A., Baquey, C. H., & Ducassou, D. (1990). Lack of responsiveness to glucose of microencapsulated islets of Langerhans after three weeks' implantation in the rat—Influence of the complement. *Journal of Microencapsulation*, *7*(3), 341–346.

Kadokawa, J., Murakami, M., & Kaneko, Y. (2008a). A facile method for preparation of composites composed of cellulose and a polystyrene-type polymeric ionic liquid using a polymerizable ionic liquid. *Composites Science and Technology*, *68*(2), 493–498.

Kadokawa, J., Murakami, M., & Kaneko, Y. (2008b). A facile preparation of gel materials from a solution of cellulose in ionic liquid. *Carbohydrate Research*, *343*(4), 769–772.

Kadokawa, J., Murakami, M., Takegawa, A., & Kaneko, Y. (2009). Preparation of cellulose–starch composite gel and fibrous material from a mixture of the polysaccharides in ionic liquid. *Carbohydrate Polymers*, *75*(1), 180–183.

Klemm, D., Heublein, B., Fink, H., & Bohn, A. (2005). Cellulose: Fascinating biopolymer and sustainable raw material. *Angewandte Chemie International Edition*, *44*(22), 3358–3393.

Li, L., Lin, Z., Yang, X., Wan, Z., & Cui, S. (2009). A novel cellulose hydrogel prepared from its ionic liquid solution. *Chinese Science Bulletin*, *54*(9), 1622–1625.

Li, Y., Wu, M., Liu, R., & Huang, Y. (2009). Cellulose-based solid–solid phase change materials synthesized in ionic liquid. *Solar Energy Materials and Solar Cells*, *93*(8), 1321–1328.

Lin, C., Wang, Y. T., & Wu, J. S. (2009). Modification in physical properties of rice gel by microbial transglutaminase. *Journal of the Science of Food and Agriculture*, *89*(3), 477–481.

Liu, C. F., Sun, R. C., Zhang, A. P., Ren, J. L., Wang, X. A., Qin, M. H., et al. (2007). Homogeneous modification of sugarcane bagasse cellulose with succinic anhydride using a ionic liquid as reaction medium. *Carbohydrate Research*, *342*(7), 919–926.

Matthew, H. W., Salley, S. O., Peterson, W. D., & Klein, M. D. (1993). Complex coacervate microcapsules for mammalian cell culture and artificial organ development. *Biotechnology Progress*, *9*(5), 510–519.

Mishra, R. K., Datt, M., Pal, K., & Banthia, A. K. (2008). Preparation and characterization of amidated pectin based hydrogels for drug delivery system. *Journal of Materials Science: Materials in Medicine*, *19*(6), 2275–2280.

Murakami, M., Kaneko, Y., & Kadokawa, J. (2007). Preparation of cellulose-polymerized ionic liquid composite by in-situ polymerization of polymerizable ionic liquid in cellulose-dissolving solution. *Carbohydrate Polymers*, *69*(2), 378–381.

Murugesan, S., & Linhardt, R. (2005). Ionic liquids in carbohydrate chemistry—Current trends and future directions. *Current Organic Synthesis*, *2*(4), 437–451.

Patel, J. D., & Chaudhuri, T. K. (2009). Synthesis of PbS/poly(vinyl-pyrrolidone) nanocomposite. *Materials Research Bulletin*, *44*(8), 1647–1651.

Prasad, K., Kaneko, Y., & Kadokawa, J. (2009). Novel gelling systems of K-, I- and λ-Carrageenans and their composite gels with cellulose using ionic liquid. *Macromolecular Bioscience*, *9*(4), 376–382.

Prasad, K., Murakami, M., Kaneko, Y., Takada, A., Nakamura, Y., & Kadokawa, J. (2009). Weak gel of chitin with ionic liquid, 1-allyl-3-methylimidazolium bromide. *International Journal of Biological Macromolecules*, *45*(3), 221–225.

Silverstein, R. M., Bassler, G. C., & Morrill, T. C. (1981). *Spectrometric identification of organic compounds*. New York: John Wiley & Sons.

Simi, C. K., & Abraham, T. E. (2010). Transparent xyloglucan–chitosan complex hydrogels for different applications. *Food Hydrocolloids*, *24*(1), 72–80.

Swatloski, R. P., Spear, S. K., Holbrey, J. D., & Rogers, R. D. (2002). Dissolution of cellulose with ionic liquids. *Journal of the American Chemical Society*, *124*(18), 4974–4975.

Wang, L., Han, G., & Zhang, Y. (2007). Comparative study of composition, structure and properties of Apocynum venetum fibers under different pretreatments. *Carbohydrate Polymers*, *69*(2), 391–397.

Wu, J., Zhang, J., Zhang, H., He, J., Ren, Q., & Guo, M. (2004). Homogeneous acetylation of cellulose in a new ionic liquid. *Biomacromolecules*, *5*(2), 266–268.

Zhang, H., Wang, Z. G., Zhang, Z. N., Wu, J., Zhang, J., & He, J. S. (2007). Regenerated-cellulose/multiwalled-carbon-nanotube composite fibers with enhanced mechanical properties prepared with the ionic liquid 1-allyl-3-methylimidazolium chloride. *Advanced Materials*, *19*(5), 698–704.

Zhang, H., Wu, J., Zhang, J., & He, J. (2005). 1-Allyl-3-methylimidazolium chloride room temperature ionic liquid: A new and powerful nonderivatizing solvent for cellulose. *Macromolecules*, *38*(20), 8272–8277.